LLNL-JRNL-2002891

Increasing the deuterated potassium dihydrogen phosphate crystal laser resistance by an additional conditioning with nanosecond pulses

W Carr, S Diop, C Miller

September 2025

Optical Engineering

Disclaimer

This work performed under the auspices of the U.S. Department of Energy by Lawrence Livermore National Laboratory under Contract DE-AC52-07NA27344.

Increasing the DKDP crystal laser resistance by an additional conditioning with nanosecond pulses

Saaxewer B. Diop*, Christopher W. Carr, Christopher F. Miller
Lawrence Livermore National Laboratory, Livermore, California, United-States

Abstract. Laser conditioning with 355-nm sub-nanosecond laser light is a well-known procedure to increase the bulk laser-induced damage resistance of DKDP crystal. In this study, we investigate a new process to further increase the bulk damage resistance of DKDP crystals by performing additional conditioning with a 6.7-ns 355-nm laser after first conditioning with a 500-ps 355-nm laser. Damage tests (using both small and large beams) show that the second nanosecond conditioning raster increased the fluence required to produce the same density (large beam test) and probability (small beam test) of bulk damage by approximately 30%.

Keywords: Laser-induced damage, DKDP crystal, Laser conditioning.

*Saaxewer Diop, diop1@llnl.gov

1 Introduction

The National Ignition Facility (NIF) achieved the first ignition on December 5, 2022 by delivering 2.05 MJ to a tritium-deuterium target.[1,2] Since this important breakthrough, numerous fusion energy projects have been launched all around the world in pursuit of future clean energy based on fusion. The NIF has since both repeated ignition and achieved more yield after increasing delivered energy to 2.2 MJ.[3] Theses results provide insight into the target physics that will be needed to continue to improve the target design and enable future fusion power plants. In order to further understand the inertial confinement fusion (ICF) reaction, more input laser energy is needed, and the objective is to increase NIF's energy output to 2.6 MJ.

As with other high-power laser facilities such as LMJ and Gekko-LFEX,[4,5] the laser-induced damage in the final optical components limits the laser input energy on target. Potassium dihydrogen phosphate (KDP), and its deuterated analog (DKDP), crystals are key components to high energy laser systems due to their ability to perform frequency conversion under relatively high fluence exposure.[6] The damage resistance of these crystals is very sensitive to the crystal growth parameters, varying significantly between crystal boules or even between regions of the boule itself. This challenge was resolved by developing laser conditioning techniques which expose crystals to slowly increasing non-damaging laser fluence.[7–12] However, as NIF continues to increase its total operating energy, these conditioning techniques are insufficient in some cases. In order to allow for higher energy density operation of KDP and DKDP crystals, we explore if a multi-pulse length laser conditioning process can be used to significantly increase the bulk damage resistance. Furthermore, we explore the impact of conditioning fluence step size and raster spatial step size during conditioning.

Adams *et al.* showed that pre-exposing KDP or DKDP crystals to 500 ps laser pulses is highly effective at increasing the bulk damage resistance of the material under subsequent exposure.[14,15] We refer to this in following sections as sub-nanosecond laser (SNL) conditioning. This study explores a new conditioning process based on an additional laser exposures after SNL-conditioning to further increase the bulk-damage resistance of DKDP crystals. Adams *et al.* performed R-on-1

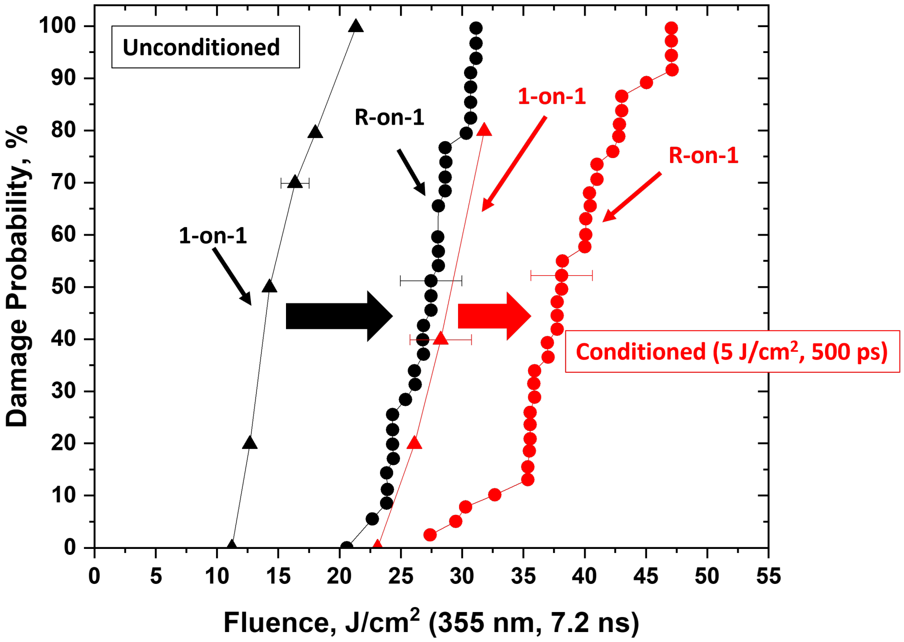

Fig 1 Damage probability as a function of the fluence measured by S-on-1 and R-on-1 tests performed on unconditioned and conditioned DKDP crystals. Adapted from Ref.[13]

damage tests on SNL-conditioned area. They demonstrated a reduction of the damage probability compared to S-on-1 (see Fig. 1), which implies the possibility of improving further the laser conditioning.[13] Based on this assumption, we first performed additional pre-exposures with a UV nanosecond laser (NL) by performing several raster-scans with a fluence ramp. Then we performed 1-on-1 tests to measure the laser damage probability and compare the laser resistance induced by the different laser conditioning process (unconditioned, SNL conditioning, and SNL + NL conditioning). We optimize the raster-scan parameters (starting fluence, fluence step, and beam overlap) to improve the additional conditioning process. Finally, we measured the damage density induced by the different laser conditioning processes with a large beam (approximately 1 cm of diameter) to have a better representation of the performance in large-scale facilities.

2 Materials

2.1 Sample description

All the data presented in this paper were obtained on a single sample. The sample was cut from a rapid growth boule with a dimension of $152.4 \times 152.4 \times 10$ mm^3. The sample was phase-matched (type II) for third harmonic generation and polished to ensure high optical quality. As received, the sample was SNL-conditioned following the procedure presented in Ref.[15] An area of the sample was left unconditioned (not exposed to laser light) in order to compare the laser resistance with the conditioned areas. No damage sites were initiated during the SNL conditioning based on bright scattering imaging.

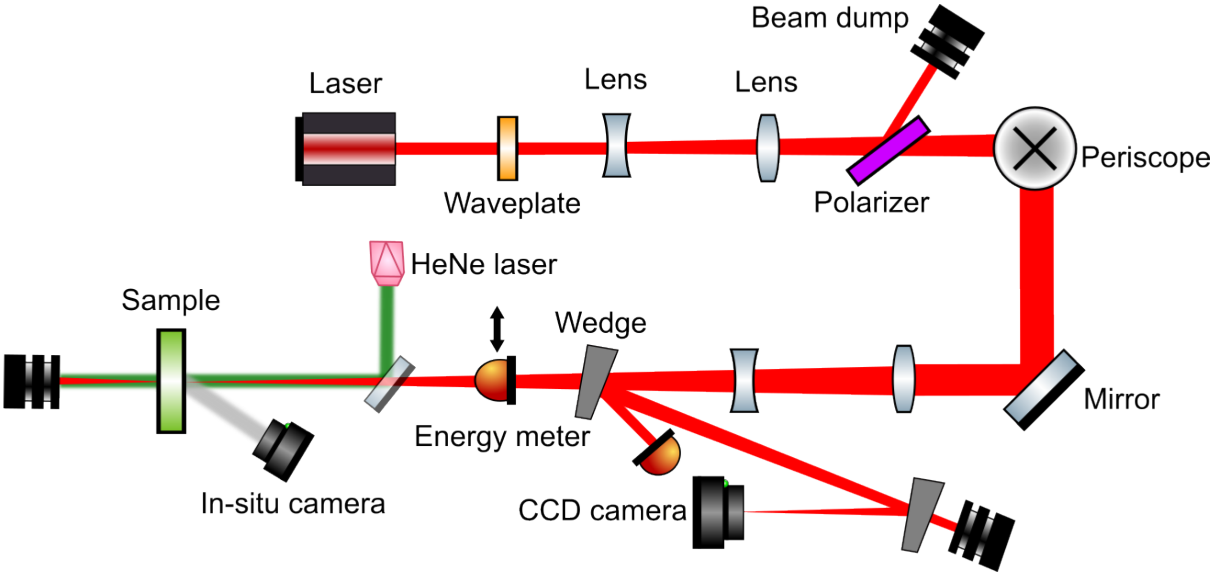

Fig 2 Schematic of the laser damage test bed dedicated to the additional conditioning and damage test experiments (1-on-1 and R-on-1).

2.2 Damage test beds and methods

Additional conditioning and laser damage tests (1-on-1 and R-on-1) were performed on the same facility described in Fig. 2. The laser source is a Nd:YAG laser system (Quanta-Ray Model PRO-350-10; Spectra-Physics, Inc., injection seeded) generating a single-longitudinal mode centered at 1064 nm (1ω), then converted to 532 nm (2ω), and 355 nm (3ω). Only the 3ω light was used in this study. The pulse duration was measured at 6.7 ns (FWHM) with a near-Gaussian temporal beam profile. Two telescopes are used to focus the beam on the sample. The first telescope (concave-convex lenses) acts as a beam expander to increase the laser-output beam size in order to obtain the desired focused beam diameter on the sample. The beam energy is regulated by a half-wave plate and a polarizer pair, which transmit the p-polarized light. A periscope rotates the polarization to vertical (s-polarized) before it is incident to the test sample. The second telescope (convex-concave lenses) focuses the beam to obtain a diameter of approximately 600 μm at $1/e^2$. A wedge samples the beam to an energy meter and a CCD camera, which is located at an equivalent focal plane as the sample. Both instruments allow us to record the energy and the spatial beam profile to measure the fluence shot-by-shot. Bulk damages are detected by using a He-Ne laser aligned co-linear to the incident 3ω beam to scatter light and detect it with a *in-situ* camera placed at an oblique incidence.

Damage density was measured in the Optical Sciences Laser (OSL) facility described in.[16] This facility offers the capability to perform damage tests with a centimeter beam and 5 ns flat-in-time (FIT) temporal pulse shape. This experiment is more representative to determine the laser resistance on a large-scale laser system.

All the experiments have been performed in s-polarization and normal incidence. Each 1-on-1 test result presented in this paper was performed using 200 sites and one shot per site (S = 1). The R-on-1 tests were performed using between 30 and 50 sites per experiment. In each case, the starting fluence was set at 5 J/cm^2, then the half-wave plate rotates with 0.5deg of increment to set a fluence ramp, using one shot per step.

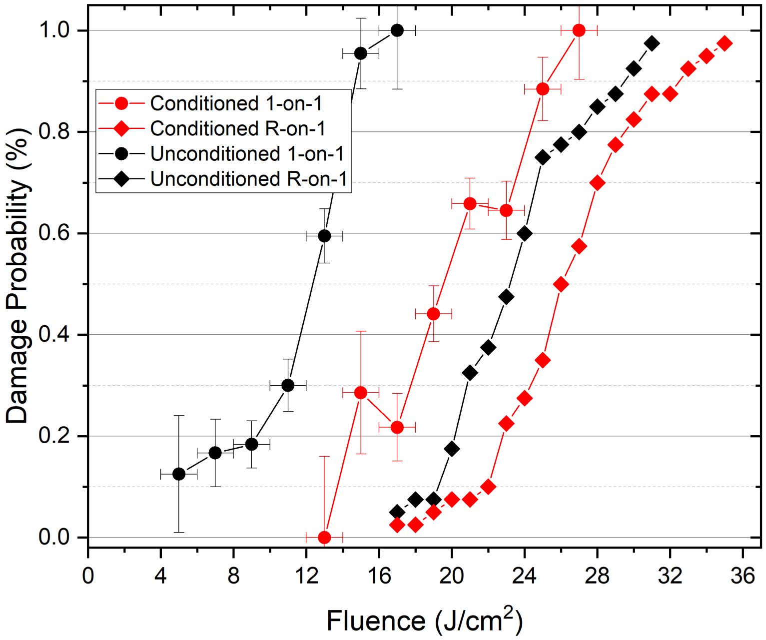

Fig 3 Damage test results of 1-on-1 and R-on-1 tests performed on unconditioned and conditioned (SNL conditioning only) areas.

3 Results

The first experiment performed was to repeat the results obtained by Adams *et al.* shown in Fig. 1. We performed 1-on-1 and R-on-1 tests on both unconditioned and SNL conditioned areas. We successively reproduced the past results; we observed an increase of the laser resistance induced by the SNL conditioning, and observed an increase of the laser resistance during the R-on-1 test on the conditioned area compared to the 1-on-1 test.

The additional conditioning procedure was based on the results obtained by Runkel *et al.*[17] They demonstrated an increase in the DKDP laser resistance after performing several raster-scans with nanosecond UV lasers (Nd:YAG and Excimer lasers). We first investigated the impact of pre-exposures at different fluences. 3 zones were defined where 3 different processes were applied. The first zone saw a single raster-scan at 6 J/cm^2, the second zone received two raster-scans at 6 then 10 J/cm^2 and the third one received three raster-scans at 6, 10, and 14 J/cm^2. The beam overlap was set at 90% of the peak fluence, which represents a step size of 150 μm. In each case, no damage sites were initiated. 1-on-1 tests were performed on each area, and the results are presented in Fig. 4. In each case, we clearly evidenced an increase of the laser resistance below the 20% of damage probability. Moreover, regarding the NIF laser resistance specification fixed at 12 J/cm^2 at 10% of damage probability, the additional conditioning represents an increase of approximately 30%. At higher fluence, the additional conditioning did not induce any reduction of the damage probability compared to the SNL conditioning.

No significant difference in bulk damage probability was noted when pre-exposing with one or three different fluences. However, we assume that the supplemental conditioning at low fluence

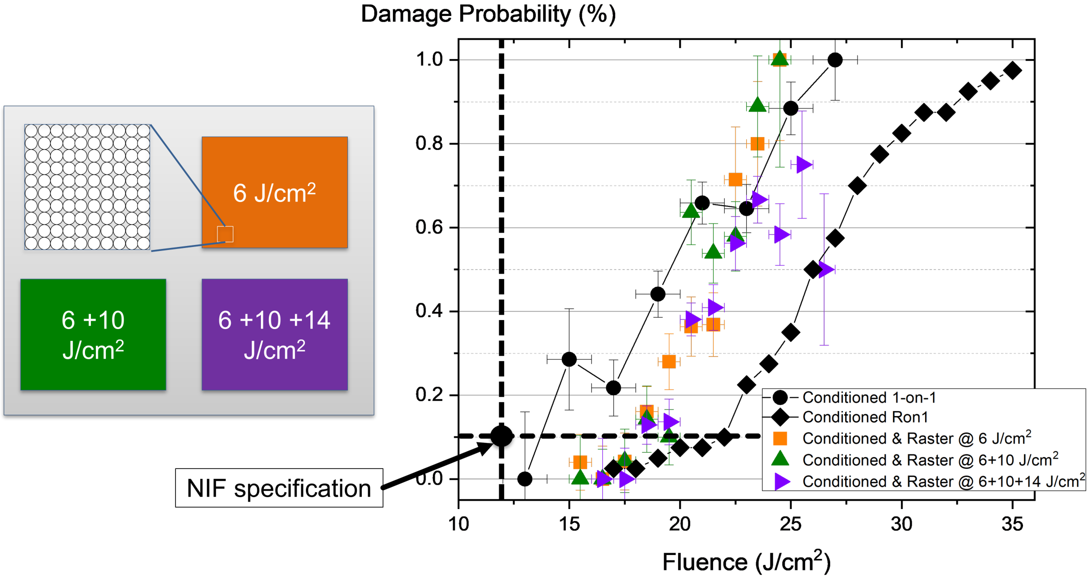

Fig 4 Damage test results after the SNL and the additional conditioning at several fluences.

(below the onset measured during the 1-on-1 tests) is important for preventing damage initiation for the raster-scans at higher fluence (above the onset). We chose to focus on performing at least three raster-scans with a fluence ramp.

To optimize the additional conditioning procedure and improve further the bulk damage resistance, several combinations of fluence and number of raster-scans were compared. The reference point is the result obtained after the supplemental conditioning performed at 6, 10, and 14 J/cm^2 (black dot in Fig. 5(b)). The step size was fixed at 150 μm for each raster-scan. Two starting fluences, 4 and 8 J/cm^2, were used and conditioning was performed up to 16 J/cm^2 (this fluence is below the onset measured through the previous R-on-1 tests). Additionally, another conditioning test (6 to 16 with a fluence ramp of 2 J/cm^2) was performed. Figure 5 shows the 1-on-1 test results; no difference in the bulk-damage resistance was observed between each case. Therefore, we conclude that the fluence step size (or the number of pre-exposures) has minimal impact on the final conditioning effect.

The effect of beam overlap during the NL laser-conditioning raster-scan was also studied. We investigated the impact of an overlap of 70%, 80% and 90% of the peak fluence overlap, which represents a step size of 240 μm, 185 μm, and 150 μm respectively. Three raster-scans were carried out at 8, 12, and 16 J/cm^2 as additional conditioning. Figure 5(a) shows performing raster-scans with 70% of beam overlap seems to be less effective than 80% and 90%. No significant difference was seen between 80% and 90% of beam overlap.

Finally, the bulk-damage density was measured with a large beam damage test.[16] A single shot was performed on the three different regions: unconditioned, SNL conditioned, and SNL + Additional NL-conditioned. The additional conditioning was performed with four raster-scans at 4, 8, 12, then 16 J/cm^2 and 90% of beam overlap. The shot on the unconditioned area was performed at an average fluence of 8 J/cm^2, while the shots on the SNL and SNL + additional conditioned areas were performed at 12 J/cm^2 on average with approximately 32% fluence contrast in both cases (see

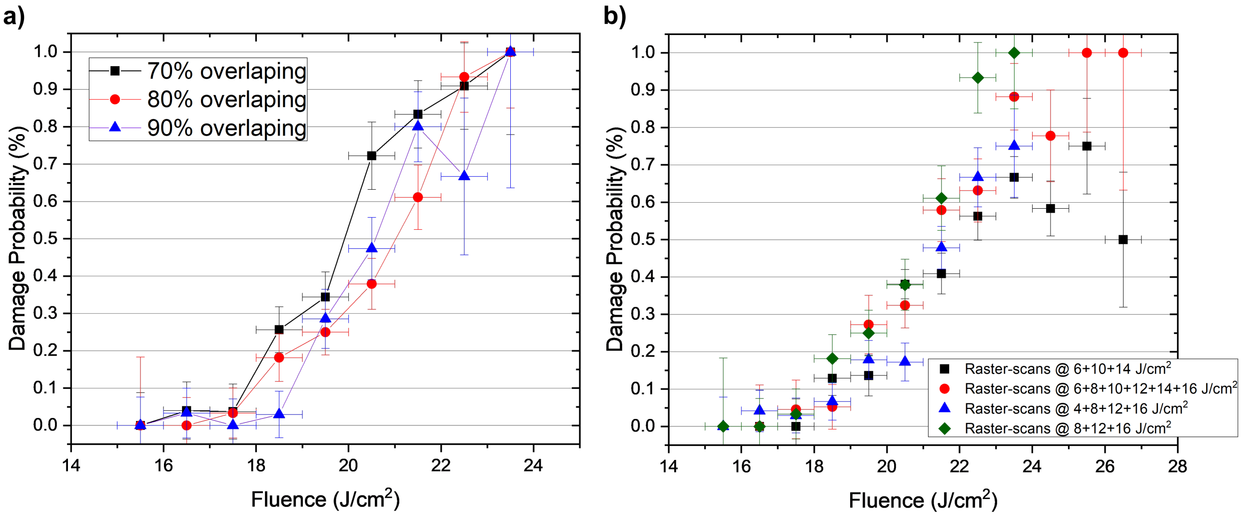

Fig 5 (a) 1-on-1 test results with different beam overlap. (b) Damage test results after the supplemental conditioning at different starting point and fluence step.

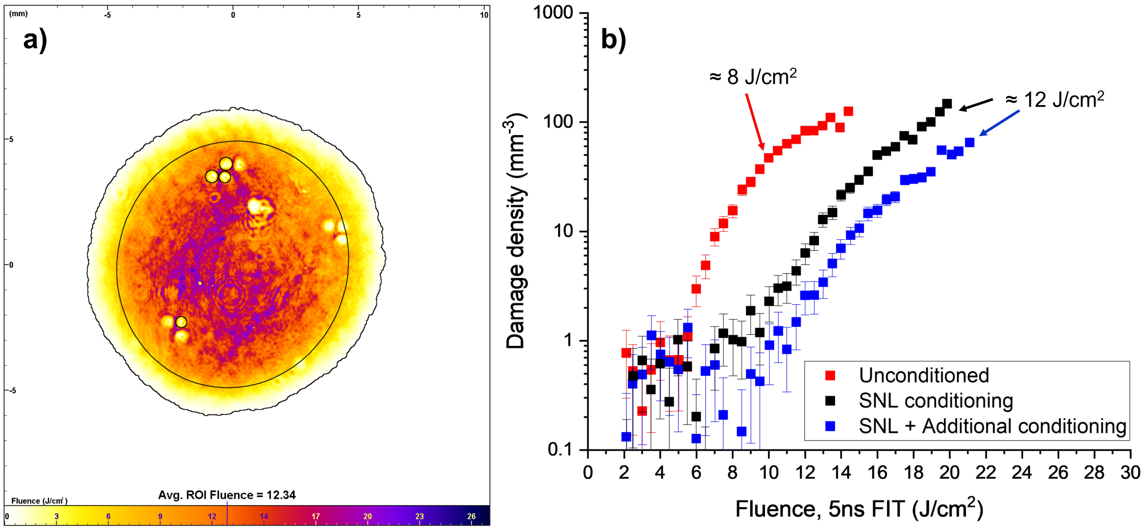

Fig 6 (a) OSL spatial beam profile at an average fluence of 12 J/cm^2. (b) Damage density measured after the OSL shot on the unconditioned, SNL-conditioned, and SNL + Additional-conditioned areas shot with average beam fluences of 8 J/cm^2, 12 J/cm^2, and 12 J/cm^2, respectively.

Fig. 6(a)). As expected, the unconditioned area was found with the highest damage density, even if the shot was at a lower fluence. Moreover, we observed a decrease of the damage density induced by the supplemental conditioning of approximately 60%. The results obtained in OSL are in good agreement with the results obtained with the small beam.

4 Conclusion

Results obtained by Adams *et al.* imply that the laser conditioning, operated at 500 ps and 355 nm, could be improved (see Fig. 1).[15] This work successfully demonstrates this effect and extends it by investigating the sensitivity of additional NL-conditioning to the parameters of fluence step size, starting fluence conditioning level, and raster step size. After the SNL conditioning, the DKDP bulk was exposed to several raster-scans with a fluence ramp with a nanosecond laser (6.7 ns) at 355 nm and 1-on-1 damage tests were performed to compare the resulting damage probability. A significant increase of approximately 30% in the crystal's bulk-damage resistance was observed by the additional conditioning (see Fig. 4). Several different variations of the additional NL laser-conditioning process were performed (fluence, fluence step, and beam overlap). We did not observe a significant impact of those parameters (see Fig. 5). Based on the damage test results, we concluded that performing various raster-scans with a fluence ramp and maximizing the beam overlap (without initiating damage sites) is the most effective procedure to increase the laser resistance. Bulk-damage density was then measured in the OSL facility. The results are in good agreement and evidenced a decrease of approximately 60% of the damage density after the additional conditioning. The next step will be to explore furthermore the additional procedure and try different laser parameters such as the pulse duration or the centered wavelength.

Disclosures

The authors declare that there are no financial interests, commercial affiliations, or other potential conflicts of interest that could have influenced the objectivity of this research or the writing of this paper.

Code, Data, and Materials Availability

The raw data and the processed data required to reproduce the findings presented in this paper can be made available upon request from the author at diop1@llnl.gov.

Acknowledgments

We thank the SNL and OSL team for assistance in the sample preparation and execution of the experiments. This work was performed under the auspices of the U.S. Department of Energy by Lawrence Livermore National Laboratory under Contract DE-AC52-07NA27344 (LLNL-JRNL-2002891).

References

1 A. L. Kritcher, D. J. Schlossberg, C. R. Weber, *et al.*, "Design of first experiment to achieve fusion target gain > 1," *Physics of Plasmas* **31**, 070502 (2024).

2 M. D. Rosen, "The long road to ignition: An eyewitness account," *Physics of Plasmas* **31**, 090501 (2024).

3 M. Durocher, V. Geppert-Kleinrath, C. R. Danly, *et al.*, "First look at neutron emission shape characteristics of ignition hotspots at the national ignition facility (invited)," *Review of Scientific Instruments* **95**, 093530 (2024).

4 J.-L. Miquel, C. Lion, and P. Vivini, "The laser mega-joule : Lmj &petal status and program overview," *Journal of Physics: Conference Series* **688**, 012067 (2016).

5 H. Shiraga, S. Fujioka, M. Nakai, *et al.*, "Fast ignition integrated experiments with gekko and LFEX lasers," *Plasma Physics and Controlled Fusion* **53**, 124029 (2011).

6 N. Zaitseva and L. Carman, “Rapid growth of kdp-type crystals,” *Progress in Crystal Growth and Characterization of Materials* **43**(1), 1–118 (2001).

7 J. Swain, S. Stokowski, D. Milam, *et al.*, “Improving the bulk laser damage resistance of potassium dihydrogen phosphate crystals by pulsed laser irradiation,” *Applied Physics Letters* **40**(4), 350–352 (1982).

8 J. Swain, S. Stokowski, D. Milam, *et al.*, “The effect of baking and pulsed laser irradiation on the bulk laser damage threshold of potassium dihydrogen phosphate crystals,” *Applied Physics Letters* **41**(1), 12–14 (1982).

9 F. Rainer, L. J. Atherton, and J. J. D. Yoreo, “Laser damage to production- and research-grade KDP crystals,” in *24th Annual Boulder Damage Symposium Proceedings – Laser-Induced Damage in Optical Materials: 1992*, H. E. Bennett, L. L. Chase, A. H. Guenther, *et al.*, Eds., **1848**, 46 – 58, International Society for Optics and Photonics, SPIE (1993).

10 L. J. Atherton, F. Rainer, J. J. D. Yoreo, *et al.*, “Thermal and laser conditioning of production and rapid growth KDP and KD*P crystals,” in *Laser-Induced Damage in Optical Materials: 1993*, H. E. Bennett, L. L. Chase, A. H. Guenther, *et al.*, Eds., **2114**, 36 – 45, International Society for Optics and Photonics, SPIE (1994).

11 M. J. Runkel, J. Bruere, W. D. Sell, *et al.*, “Effects of pulse duration on bulk laser damage in 350-nm raster-scanned DKDP,” in *Laser-Induced Damage in Optical Materials: 2002 and 7th International Workshop on Laser Beam and Optics Characterization*, G. J. Exarhos, A. H. Guenther, N. Kaiser, *et al.*, Eds., **4932**, 405 – 414, International Society for Optics and Photonics, SPIE (2003).

12 P. DeMange, C. W. Carr, R. A. Negres, *et al.*, “Multi-wavelength investigation of laser-damage performance in kdp and dkdp following laser annealing,” *Optics Letters* **30** (2004).

13 J. J. Adams, J. A. Jarboe, M. D. Feit, *et al.*, “Comparison between S/1 and R/1 tests and damage density vs. fluence (Rho(Phi)) results for unconditioned and sub-nanosecond laser-conditioned KD2PO4 crystals,” in *Laser-Induced Damage in Optical Materials: 2007*, G. J. Exarhos, A. H. Guenther, K. L. Lewis, *et al.*, Eds., **6720**, 672014, International Society for Optics and Photonics, SPIE (2007).

14 J. J. Adams, T. L. Weiland, J. R. Stanley, *et al.*, “Pulse length dependence of laser conditioning and bulk damage in KD2PO4,” in *Laser-Induced Damage in Optical Materials: 2004*, G. J. Exarhos, A. H. Guenther, N. Kaiser, *et al.*, Eds., **5647**, 265 – 278, International Society for Optics and Photonics, SPIE (2005).

15 J. J. Adams, J. A. Jarboe, C. W. Carr, *et al.*, “Results of sub-nanosecond laser-conditioning of KD2PO4 crystals,” in *Laser-Induced Damage in Optical Materials: 2006*, G. J. Exarhos, A. H. Guenther, K. L. Lewis, *et al.*, Eds., **6403**, 64031M, International Society for Optics and Photonics, SPIE (2007).

16 M. C. Nostrand, T. L. Weiland, R. L. Luthi, *et al.*, “A large-aperture high-energy laser system for optics and optical component testing,” in *Laser-Induced Damage in Optical Materials: 2003*, G. J. Exarhos, A. H. Guenther, N. Kaiser, *et al.*, Eds., **5273**, 325 – 333, International Society for Optics and Photonics, SPIE (2004).

17 M. J. Runkel, K. P. Neeb, M. C. Staggs, *et al.*, “Results of raster-scan laser conditioning studies on DKDP triplers using Nd:YAG and excimer lasers,” in *Laser-Induced Damage in Optical Materials: 2001*, G. J. Exarhos, A. H. Guenther, K. L. Lewis, *et al.*, Eds., **4679**, 368 – 383, International Society for Optics and Photonics, SPIE (2002).

Saaxewer Diop graduated from Ecole Centrale Marseille, France, with a Ph.D. in optics, photonics and image processing. He participated in the development of the LMJ-PETAL facility at the French Atomic and Alternative Energies Commission (CEA). He studied the laser damage growth phenomenon on PETAL's dielectric transport mirrors. In addition, he has worked on the design and optimization of the laser resistance of the pulse compression gratings of PETAL. He is currently a post-doctoral researcher at the Lawrence Livermore National Laboratory. His current research focuses on identifying and mitigating laser-induced damage mechanisms on NIF optical components.

Biographies and photographs of the other authors are not available.

List of Figures

List of Tables